

doi:10.15199/48.2022.09.02

# A module for analysis of power supplies of an electronic security systems

**Abstract.** The article deals with a detailed description of a module for monitoring and analysis of electronic security systems supplies design. The module contains modern microprocessor technology, simple but relatively new methods of measuring key electrical quantities, ergonomic control, a modern display unit and communication technology with an environment. As a proof of the functionality and especially accuracy of the measurement, the dependences of relative measurement errors of important electrical quantities on their true values were chosen.

**Streszczenie.** Artykuł dotyczy szczegółowego opisu modułu do monitorowania i analizy projektowania dostaw elektronicznych systemów zabezpieczeń. Moduł zawiera nowoczesną technologię mikroprocesorową, proste, ale stosunkowo nowe metody pomiaru kluczowych wielkości elektrycznych, ergonomiczne sterowanie, nowoczesny wyświetlacz oraz technologię komunikacji z otoczeniem. Jako dowód funkcjonalności, a zwłaszcza dokładności pomiaru, wybrano zależności względnych błędów pomiarowych ważnych wielkości elektrycznych od ich rzeczywistych wartości. (Moduł do analizy zasilaczy elektronicznych systemów zabezpieczeń)

**Keywords:** voltage measurement, current measurement, microcontroller system, relative error analysis.

**Słowa kluczowe:** pomiar napięcia, systemy zabezpieczeń

## Introduction

Currently, there is significant development of electronic security systems, which serve to signalize presence of an intruder in the technologies of protection of possession and persons, so that competent units can respond adequately. These systems are used to protect a perimeter, a shell of important buildings, to signalize a movement of unwanted people in important buildings and to protect valuable objects. These technologies are becoming more complex and sophisticated. Reliable power supplies are required to ensure proper operation of the entire system. The power supply must safely cover the highest load of the entire system, or ensure a switching to backup power supply and the required signaling. Current power supply systems therefore need to be monitored, it is need to measure important parameters and carefully evaluate [1, 2]. The article is devoted to the module for analysis of power supply systems in technologies for protection of possession and persons. This article is based on the diploma thesis.

## Design of a module for analysis of power supply systems

Direct current power supplies are mainly used to power electronic circuits of individual subsystems of electronic security system, therefore the above mentioned module is designed for these systems. Reconnaissance of the market with the most frequently used power supplies in the field of electronic security systems was performed and monitored parameters were selected on the basis of this. Important electrical parameters that were taken into account were output DC voltage, current and power. The most common output voltage is 12 V, in the case of regulation 12 - 14 V. The minority representation is 24 V, in the case of regulation 24 - 28 V. In rare cases, it is possible to meet supplies with an output voltage of 36 - 48 V. A very important power supply parameter, which can be used to determine how large system will cover, is output current. This is most often in the range of 1 - 10 A. In a smaller representation, the current is above 10 A to 20 A [3]. If the power supply uses voltage of 12 V and is needed to allow a load of 20 A, the power of 240 W corresponds to the power supply. The designed module is therefore devised for the most commonly used power supplies. The range of output voltage 12.0 - 13.8 V and output current 0 - 10 A was considered. It was determined that the module will monitor, evaluate and display actual voltage in the range of 8 - 16 V,

current in the range of 0 - 20 A, power which supply provides to the system and the consumption of the given electronic security system. Furthermore, the module ensures setting of maximum and minimum values of voltage and current, signalizes or highlights their exceeding or falling over or below the set limit. The module also saves the measured values on a storage medium and is also able to select a frequency of the measured samples. It is powered from an analyzed supply. The module is compact, allows easy replacement or addition of important elements and easy configuration. The block diagram of the designed module as a part of the electronic security system is shown in Fig. 1.

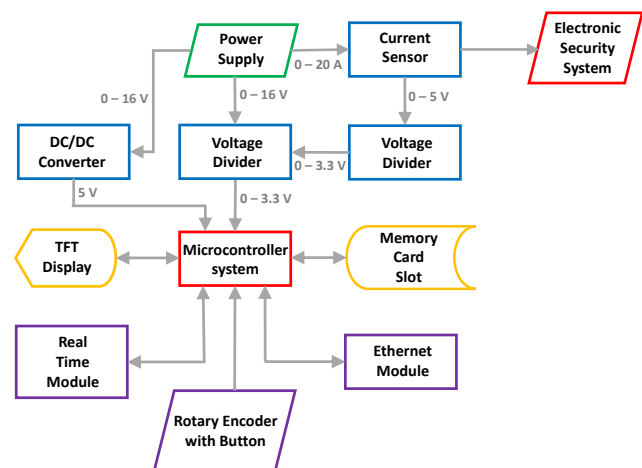


Fig. 1. The block diagram of the designed module

The core of this module is ARDUINO DUE, which has ATSAM3X8EAU processor with ARM architecture [4]. This processor system provides measurement of key quantities, calculations and control of the entire module. The device is designed as modular system. The printed circuit board of the other accessories of the device is connected to this processor system as another module. The device also contains DC/DC converter TSR1-2450 from Traco Power company, whose output voltage is 5 V and allows output current of up to 1 A. It is used to supply the processor system and other accessories. The advantage of this component is that it has very stable output voltage, it can be connected to the DC voltage in wide range of 5.5 - 36 V, no

external components are needed except of a capacitor with capacitance of 22  $\mu\text{F}$  at the input in case of higher voltage [5]. This component also does not heat up even at the maximum output current. Another big advantage is its availability at the market. Another important part is a measurement system of key variables. Voltage and current were considered as key variables. A voltage divider was chosen as the voltage sensor [6]. There are more modern methods for measuring voltage. One of the modern methods is usage of a non-contact voltage sensor, which is mentioned in [7]. However, this method is more technologically complex, so this simple and effective method was used here. It was supposed that the maximum measured voltage value will be 16 V. From this the design of the divider was derived. The voltage divider ensures that the voltage is reduced to the maximum value of 3.3 V, which is the value with which the applied processor system can operate. The voltage divider is shown in Fig. 2.

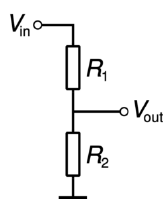


Fig. 2. Voltage divider

Then digitization takes place. The measured voltage value is then defined by relation (1).

$$(1) \quad V_{in} = (U_{ref}/resolution) \cdot x \cdot ((R_1 + R_2)/R_2),$$

where:  $V_{in}$  - measured voltage value,  $U_{ref}$  - voltage reference value,  $resolution$  - microprocessor system resolution,  $x$  - converted digital value of  $V_{out}$  stored in a variable in the microprocessor system,  $R_1$  - resistance size of the first divider resistor,  $R_2$  - resistance size of the second divider resistor.

The reference voltage value was considered to be 3.3 V, with which the given processor system works. The  $resolution$  value is 4095, which is again available in the processor system. The resistance size of resistor  $R_1$  was 47100  $\Omega$  and the resistance size of resistor  $R_2$  was 180200  $\Omega$ . These are true resistance values of the applied resistors measured by the Pro'sKit<sup>®</sup> MT-1707 multimeter [8].

The integrated current sensor ACS715LLCTR-20A-T from Allegro MicroSystems company in a surface mount design was used for current measurement. This current sensor uses a relatively new method of current measurement using the Hall effect [9, 10, 11]. The Hall voltage is proportional to the measured current. This integrated sensor allows to measure current in the range of 0 - 20 A. The voltage output is in the range of 0.5 - 5.0 V. The disadvantage of this sensor is certain voltage value at zero current, in this case it is 0.5 V [12]. However, this can be easily eliminated by calculation in a microprocessor system. Before the voltage output value is digitized, it is necessary to reduce the value, which is connected to the input of the processor system, to the maximum value of 3.3 V. This again provides a voltage divider in the similar way as in the previous part. The value of the measured current is then defined by relation (2).

$$(2) \quad I = ((U_{ref}/resolution) \cdot x \cdot ((R_1 + R_2)/R_2) - 0.5) \cdot (1/sens),$$

where:  $I$  - measured current,  $U_{ref}$  - voltage reference value,  $resolution$  - processor system resolution,  $x$  - converted

digital value of the voltage divider output stored in the processor system variable,  $R_1$  - resistance size of the first divider resistor,  $R_2$  - resistance size of the second divider resistor, 0.5 - voltage value at zero current,  $sens$  - voltage to current conversion constant.

The resistance size of the resistor  $R_1$  was 62100  $\Omega$  and the resistance size of the resistor  $R_2$  was 120300  $\Omega$ . These are the true resistance values of the applied resistors, again measured with the Pro'sKit<sup>®</sup> MT-1707 multimeter. The voltage to current conversion constant is 185 mV/A [12].

Since the measured current value is taken in account up to 20 A, which allows the selected integrated sensor, it was necessary to correctly dimension the printed circuit board path for part of the measured current. It is based on current density. The value of the current density at which the path on the printed circuit board can be permanently loaded without blowing or significantly heating is 100 A/mm<sup>2</sup>. The most commonly used copper layer thickness on a printed circuit board is 35  $\mu\text{m}$  [13]. Then the path width on the printed circuit board is defined by relation (3).

$$(3) \quad d = I/(J \cdot h),$$

where:  $d$  - path width on the printed circuit board,  $I$  - value of the maximum measured current,  $J$  - mentioned current density,  $h$  - thickness of the copper layer on the printed circuit board.

The path width on the printed circuit board was calculated to be 5.71 mm. The value of 6.00 mm was chosen to secure the reserve.

The real-time module with DS1307 [14] chip was used to assign a time trace to the samples of individual measurements. This module provides real time with leap year correction. It communicates with the processor system via the I2C interface.

The MSP3520 TFT resistive touch screen with ILI9488 [15] driver was used to display value setting, monitored values and time. This display unit therefore also allows the control of the complete module. In case of the touch screen failure, the EC11 rotary encoder with button [16] was also implemented to control the module.

The device also contains a memory card slot for storing the module configuration and also for storing monitored data.

The trend of modern electronic security systems is the support of their configuration, control and access to data via TCP/IP and HTTP/HTTPS protocols, therefore the module is equipped with the Ethernet interfaceUSR-ES1 W5500 [17]. This interface communicates with the processor system via the SPI bus. The design of the proposed module is shown in Fig. 3.



Fig. 3. Photo of the proposed module

#### Algorithm in the microprocessor system

The algorithm in the microprocessor system was based on the above-mentioned specification of the module

function and menu structure in the control system. Thus the following capabilities of the proposed module were determined: displaying of the measured voltage, current, power, consumption and their storage on a memory card, setting of the maximum and minimum value of the measured voltage and current, when exceeding the maximum value of voltage and current differentiation in red text and recording this fact on a memory card, when the voltage and current value drop below the set limit differentiation of yellow text and recording this fact on a memory card, module setting using the configuration file on a memory card, setting date and time, touch screen calibration, reading the configuration file from a memory card or EEPROM, ability to software connect or disconnect a memory card, and ability to save or load a configuration file from a memory card. The flow chart of the complete algorithm in the microprocessor system of the designed module is shown in Fig. 4.

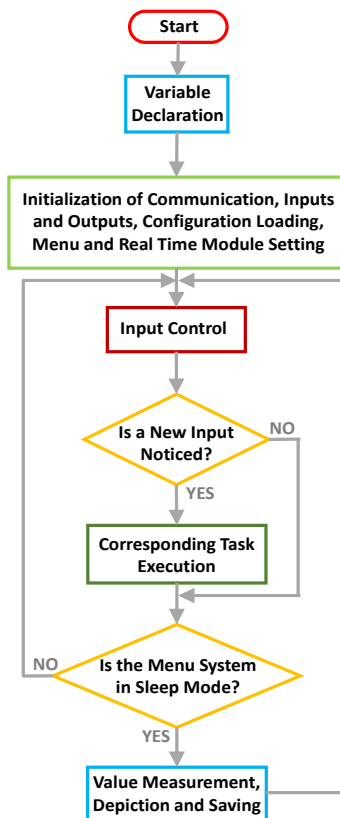


Fig. 4. Flow chart of the algorithm

The algorithm initially declares all necessary variables. This is followed by initialization of communication via the already mentioned interfaces, setting of input and output ports, loading of configuration from EEPROM or memory card, setting of system menu and functions of real time module. The program then tests all individual inputs. If an action is detected on any input, it performs the required task. If no action is recorded, the system menu continues. When the system menu is in sleep mode, key values are measured, calculated, the values are displayed and stored on a memory card. If the system menu is not in sleep mode, the program will return before the operation of checking individual inputs. And this algorithm is constantly repeated.

#### Function verification of the designed and manufactured module

As part of verification of correct function of the designed and manufactured module, all items of the system menu as well as individual parts of the module were tested. This

module is primarily intended for measuring key quantities, such as voltage and current, which are then needed for further calculations and analysis of power supplies of electronic security systems. Thorough testing was therefore focused on evaluating of accuracy of measuring just these quantities. As a proof of the accuracy of the measurement, dependence of relative error of appropriate quantity on its true value was shown. The block diagram of the measuring workplace is shown in Fig. 5.



Fig. 5. Block scheme of the measuring workplace

The laboratory power supply QPX1200S AIM-TTI [18] was used as the power system for testing, which provided maximum output voltage of 60 V and maximum output current of 50 A. A laboratory load was used as a simulation of an electronic security system, which supported voltage up to 200 V and current consumption up to 20 A. First, initial dependence of relative error of current measurement on its true value was discovered. True current was setting on the laboratory supply from 0.09 A, which is the consumption value of the designed module, in steps of 0.50 A to 12.00 A. The measured current values depicted on the display of the designed module were monitored, recorded and relative measurement errors computation was performed. The dependence of relative error of current measurement on its true value is illustrated in Fig. 6.

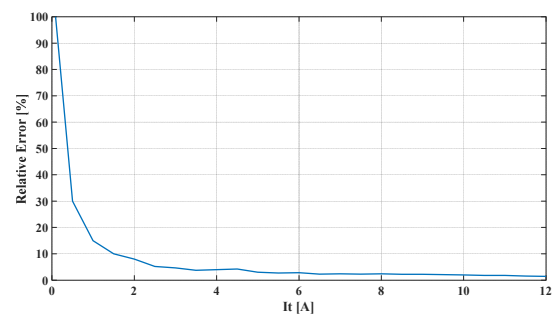


Fig. 6. Dependence of relative error of current measurement on its true value

From the initial measurement, it can be seen that the highest relative error is at set actual current, which is close to 0.00 A. As the current increases, the relative error of the measurement decreases rapidly. Important statistical indicators were calculated for this course. The minimum relative error was 1.42%, the maximum relative error reached 100.00% and mean relative error was 8.72%. These statistic parameters indicate that the current measurement error was high, so a correction was performed to the current measurement. The mean value of the absolute current measurement error, which was 0.1652 A, was used for the correction. This value was then used in the calculation of the corrected measured current value in the microprocessor system. The dependence of the relative error on its true value after correction is shown in Fig. 7. The original characteristic for comparing of correction quality is also shown here.

From this characteristic it can be seen that after the correction in the microprocessor system, the designed module significantly refined the current measurement in the whole range. The relative measurement error is significantly smaller than in the previous case. This is most evident at lower current values. Here again, important statistical

indicators were calculated. The minimum relative error reached 0.00%, the maximum relative error was 1.11% and the mean relative error was 0.67%. Indeed, these values prove that the current measurement is significantly more accurate. The minimum value of relative error decreased by 1.42%, the maximum relative error even decreased by 100.00% and the mean value of relative error decreased by 7.61%.

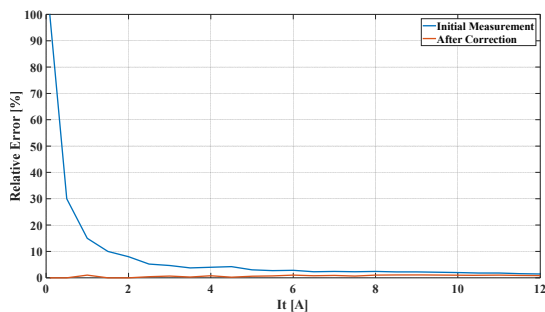


Fig. 7. Dependence of relative error of current measurement on its true value after correction

This was followed by verification of accuracy of the voltage measurement by the designed module. The module was designed to monitor voltage close to 12 V. Verification of accuracy of voltage measurements was performed in such a way that another laboratory power supply was connected via the designed module to the above mentioned laboratory electronic load. The LW-K3010D [19] power supply, which allows the output voltage 30 V and current 10 A, was chosen for this testing. The voltage of 12 V was set on the laboratory power supply and the current from 0.08 A to 10.00 A was set with an electronic load in step of 0.50 A and the voltage measured by the designed module was monitored and recorded. The data displayed on the electronic load was used as true voltage value. Subsequently, relative measurement errors were calculated. The initial value of 0.08 A was actual current value consumed by the designed module. The dependence of the relative voltage error on the true value of the initial measurement before correction is shown in Fig. 8.

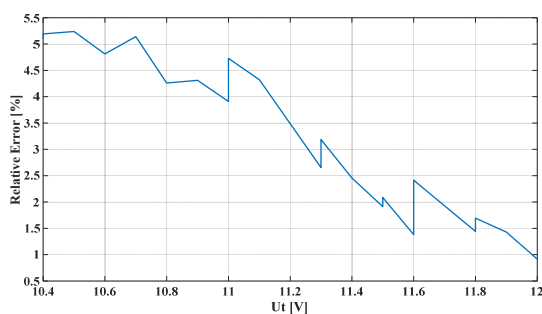


Fig. 8. Dependence of relative error of voltage measurement on its true value

From the initial voltage measurement, it can be concluded that the proposed module shows higher relative errors at lower values of the measured voltage. The lowest value of relative error is at measured voltage of 12 V. Important statistical parameters were also analyzed for this quantity. The minimum value of relative error here was 0.92%, the maximum value of relative error was 5.24% and the mean value of relative error here was 3.27%. The initial voltage measurement again showed relatively high values of relative errors, although not as high as in the case of current measurements. Again, it was necessary to make a correction using mean value of absolute error, which was 0.3586 V. The correction was also made by computation in

the microprocessor system of the module. The dependence of the relative error of the voltage measurement on its true value after correction is shown in Fig. 9. The original characteristic for comparison is also depicted here.

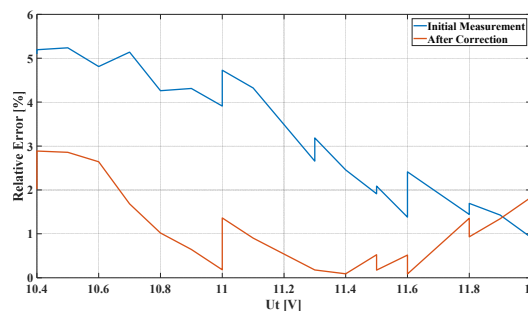


Fig. 9. Dependence of relative error of voltage measurement on its true value after correction

From the above characteristics, it can be again seen that after correction in the microprocessor system, the designed module shows much smaller relative voltage measurement errors. However, when measuring voltage on the value of 12 V, the relative error is greater. Again, important statistical indicators were calculated. The minimum value of relative error was 0.09%, the maximum value of relative error was 2.88% and the mean value of relative error was 1.11%. The correction in the module's microprocessor system therefore significantly improved the voltage measurement. The minimum relative error was reduced by 0.83%. The maximum value of relative error decreased by 2.36% and the mean value of relative error decreased by 2.16%.

From these basic quantities, the current supply power and consumption of an electronic security system, were then calculated in the microprocessor system. The photo of the real workplace, where all tests of functionality and measurement accuracy of the designed module were performed, is shown in Fig. 10.



Fig. 10. Workplace for testing

The calculation of current power of supply system defines relation (4).

$$(4) \quad P_s = U_m \cdot I_m,$$

where:  $P_s$  - current power of supply of electronic security system,  $U_m$  - measured voltage by the module,  $I_m$  - measured current by the module.

For consumption of electronic security system, it was necessary to measure its operating time. The operating time of the system was also determined in the

microprocessor via the real time module. The calculation of the consumption of electronic security system defines the relation (5).

$$(5) \quad W_{ESS} = P_s t_{ESS},$$

where:  $W_{ESS}$  – is consumption of electronic security system,  $P_s$  - current power of electronic security system,  $t_{ESS}$  - operating time of electronic security system.

An example of visualization of monitored data is shown in Fig. 11.



Fig. 11. Visualization of monitored data

## Conclusion

The article dealt with complete design of the module for monitoring and analysis of power supplies of an electronic security system. This module allows easy addition of other accessories, uses modern processor system, display unit and the latest wire technologies to communicate with an environment, implements simple but still current technologies for measuring key electrical quantities and is designed so that it can be easily installed in existing power supply system's housing. To verify the accuracy of the measurements and especially the accuracy of the key quantities, the dependences of the relative errors of the individual quantities on their true value were calculated. The correction of measured values was performed by computation in the microprocessor system. This correction significantly improved the measurements, which is represented by the above mentioned values of relative errors. The maximum relative error of current measurement dropped from 100.00% to 1.11%. The minimum relative error of current measurement dropped from 1.42% to 0.00%. The maximum relative error of voltage measurement dropped from 5.24% to 2.88%. The minimum relative error of voltage measurement dropped from 0.92% to 0.09%. The current measurement is better corrected in the microprocessor system than voltage measurement. Current is very important to analyze consumption of an electronic security system.

The future aim for working on this issue could be to equip this module with wireless technologies for communication with surrounding systems and configuration of the module. Such wireless technologies could be Bluetooth, WiFi or GSM network.

*The work presented in this article was supported by the Czech Republic Ministry of Defence – University of Defence Development Program – “Conduction of Operations in Airspace” and the Czech Republic Ministry of Education, Youth and Sports – University of Defence student research program “Modern Methods of Generation, Direction Control and Signal Processing”.*

**Authors:** Ing. Přemysl Janů, Ph.D., University of Defence, Department of Communication Technologies, Electronic Warfare and Radiolocation, Kounicova 65, 662 10, Brno, E-mail: [premysl.janu@unob.cz](mailto:premysl.janu@unob.cz); Ing. Šimon Brázda, University of Defence, Department of Combat and Special Vehicles, Kounicova 65, 662 10, Brno, E-mail: [simonbrazda@seznam.cz](mailto:simonbrazda@seznam.cz); Barbora Odvárková, University of Defence, Department of Communication Technologies, Electronic Warfare and Radiolocation, Kounicova 65, 662 10, Brno, E-mail: [barbora.odvarkova@unob.cz](mailto:barbora.odvarkova@unob.cz).

## REFERENCES

- [1] Jakubowski K., Paś J., Określenie parametrów eksploatacyjnych wybranych elektronicznych systemów bezpieczeństwa na podstawie procesu ich użytkowania w obiektach infrastruktury krytycznej, *Przegląd Elektrotechniczny*, 97 (2021), nr 10, 103-109
- [2] Jakubowski K., Paś J., Rosinski A., The Issue of Operating Security Systems In Terms of the Impact of Electromagnetic Interference Generated Unintentionally, *Energies*, 2021, nr 14 (24), 1-17
- [3] Brázda Š. A Module for Power Supply Analysis of Electronic Security Systems, Diploma Thesis, 2021, available from: [https://github.com/SimonBrazda/Diploma\\_thesis-EZS\\_PSU\\_Monitor](https://github.com/SimonBrazda/Diploma_thesis-EZS_PSU_Monitor)
- [4] ARDİNO DUE, 2022, available from: <https://store.arduino.cc/products/arduino-due>
- [5] TSR 1-2450, 2022, available from: <https://www.tracopower.com/int/model/tsr-1-2450>
- [6] Voltage Divider Formula, 2022, available from: <https://www.toppr.com/guides/physics-formulas/voltage-divider-formula/>
- [7] Delle Femine A., Gallo D., Landi C., Lo Schiava A., Luiso M., Low Power Contactless Voltage Sensor for Low Voltage Power Systems, *Sensors*, 19 (2019), nr 16, 1-16
- [8] MT-1707, 2022, available from: <https://www.digikey.com/en/products/detail/eclipse-tools/MT-1707/15779957>
- [9] Janů P., Jalovecký R., Proposal of Power Supply Monitoring Unit with CANaerospace Protocol, International Conference on Electrical Systems for Aircraft, Railway and Ship Propulsion, Bologna, Italy, 2010, 1-5
- [10] Crescentini M., Ramilli R., Gibiino G. P., Marchesi M., Canegallo R., Romani A., Tartagni M., Traverio P. A., The X Hall Sensor: Toward Integrated Broadband Current Sensing, *IEEE Transactions on Instrumentation and Measurement*, 70 (2021), 1-12
- [11] Ajbl A., Pastre M., Kayal M., A Fully Integrated Hall Sensor Microsystem for Contactless Current Measurement, *IEEE Sensors Journal*, 13 (2013), nr 6, 2271-2278
- [12] ACS 715, 2022, available from: <file:///C:/Users/janup/AppData/Local/Temp/ACS715-Datasheet.pdf>
- [13] PCB Trace Width Calculator, 2022, available from: <https://www.mclpcb.com/blog/pcb-trace-width-vs-current-table/>
- [14] DS1307, 2022, available from: <https://datasheets.maximintegrated.com/en/ds/DS1307.pdf>
- [15] 3.5inch SPI Module ILI9488 SKU: MSP3520, 2022, available from: [http://www.lcdwiki.com/3.5inch\\_SPI\\_Module\\_ILI9488\\_SKU:MS P3520](http://www.lcdwiki.com/3.5inch_SPI_Module_ILI9488_SKU:MS P3520)
- [16] EC11, 2022, available from: <https://www.farnell.com/datasheets/1837001.pdf>
- [17] Durable Electronics USR-ES1 W5500 Chip SPI to LAN/Ethernet Converter TCP/IP Mod, 2022, available from: <https://www.walmart.com/ip/Durable-Electronics-USR-ES1-W5500-Chip-SPI-to-LAN-Ethernet-Converter-TCP-IP-Mod/681626200>
- [18] QPX1200SP, 2022, available from: [https://octopart.com/qpx1200sp-aim-tti-instruments-19799339?gclid=EAlaIqobChMli5imypOY9gIVi7d3Ch3i\\_wPpEAAAYAAEgKHH\\_D\\_BwE](https://octopart.com/qpx1200sp-aim-tti-instruments-19799339?gclid=EAlaIqobChMli5imypOY9gIVi7d3Ch3i_wPpEAAAYAAEgKHH_D_BwE)
- [19] LW-K3010D 0-30V/0-10A, 2022, available from: <https://www.hadex.cz/g853-laboratorni-zdroj-lw-k3010d-0-30v0-10a/>